Cite this article
Muthukumar N, Arumugam H, Krishnasamy B, Muthusamy A and Muthukaruppan A (2024) Flame-retardant and anti-corrosion behaviour of cardanol-based polybenzoxazine composites. *Green Materials* **12(1)**: 3–14, https://doi.org/10.1680/jgrma.22.00020

Research Article
Paper 2200020
Received 24/02/2022; Accepted 03/07/2023
First published online 05/07/2023

Green Materials

Flame-retardant and anti-corrosion behaviour of cardanol-based polybenzoxazine composites

Narmatha Muthukumar MSc, MPhil
Polymer Engineering Laboratory, PSG Institute of Technology and Applied Research, Coimbatore, India; Post Graduate and Research Department of Chemistry, Sri Ramakrishna Mission Vidyalaya College of Arts and Science, Coimbatore, India; Assistant Professor, Department of Chemistry, SNS College of Technology, Coimbatore, India

Hariharan Arumugam PhD
Assistant Professor, Polymer Engineering Laboratory, PSG Institute of Technology and Applied Research, Coimbatore, India

Balaji Krishnasamy PhD
Associate Professor, Polymer Engineering Laboratory, PSG Institute of Technology and Applied Research, Coimbatore, India

Athianna Muthusamy PhD
Associate Professor, Post Graduate and Research Department of Chemistry, Sri Ramakrishna Mission Vidyalaya College of Arts and Science, Coimbatore, India

Alagar Muthukaruppan PhD
Professor, Polymer Engineering Laboratory, PSG Institute of Technology and Applied Research, Coimbatore, India (corresponding author: muthukaruppanalagar@gmail.com)

A new monomer of bi-functional benzoxazine was synthesised using cardanol (C) and *p*-phenylenediamine (*p*pda) under suitable experimental conditions. The curing behaviour of the cardanol-based 1,4-bis(7-pentadecyl-2*H*-benzo[1,3]oxazin-3(4*H*)-yl)benzene (C-*p*pda) benzoxazine monomer was studied by differential scanning calorimetry analysis, and the polymerisation temperature (T_p) of C-*p*pda benzoxazine was found to be 237°C. Further, the benzoxazine monomer was reinforced with varying weight percentages (5, 10 and 15 wt%) of bio-ash derived from *Aerva lanata* (AL-ash) to obtain hybrid composites. Thermogravimetric analysis data indicate that AL-ash-reinforced benzoxazine composites possess excellent thermal stability and a flame-retardant behaviour. The morphology of AL-ash- and cardanol-based benzoxazine composites was analysed using field emission scanning electron microscopy (FESEM). The FESEM results indicate homogeneous distribution of AL-ash in the composites. Energy-dispersive X-ray spectroscopy analysis was used to determine the elemental composition of the AL-ash used for the preparation of composites. The value of the water contact angle of poly(C-*p*pda) was found to be 148°. Data obtained from corrosion studies indicate that the mild steel specimen coated with a benzoxazine matrix and the specimen coated with bio-ash-reinforced benzoxazine composites exhibit an excellent resistance against corrosion. The bio-ash-reinforced composites of cardanol-based benzoxazine can be used in the form of sealants, encapsulants, adhesives, coatings and matrices in microelectronics and automobile applications under high thermal and moist environmental conditions.

Keywords: *Aerva lanata* ash/bio-benzoxazine composites/contact angle/corrosion/hydrophobic

Notation

C_{dl}	coating capacitance
E_{corr}	corrosion potential
F	Faraday constant
I_{corr}	corrosion current density (A/cm^2)
M	molecular mass of copper
n	number of electrons transferred during the corrosion reaction
n_{dl}	constant phase element
R_c	coating resistance
R_{ct}	charge-transfer resistance
R_s	solution resistance
T_{dmax}	maximum degradation temperature
T_p	polymerisation temperature
$Y_{0,dl}$	admittance of polymer coating and electrolytic solution interface
β_a, β_c	Tafel constants for anodic and cathodic polarization regions, respectively
θ	percentage char yield of materials at 850°C
ρ	density of the mild steel specimen

1. Introduction

Polybenzoxazines are one of the most important and versatile classes of modified high-performance phenolic thermosetting polymers;[1] they possess good mechanical properties,[2] good thermal properties,[3] a low moisture uptake, a high carbon residue, a good flame-retardant behaviour,[4] low surface free energy and excellent dielectric properties.[5–7] These properties make them useful as sealants in electronic device fabrication,[8] adhesives,[9] coatings and composites for different industrial and engineering applications. However, conventional polybenzoxazines (bisphenol A, bisphenol F etc.) are prepared from petroleum products, which have some shortcomings such as brittleness and a high polymerisation temperature. To overcome these drawbacks and to reduce the consumption of fast-depleting petroleum products,[10,11] the development of bio-benzoxazine-based composites with varying skeletons and high-performance properties is warranted.[12–15]

A class of bio-polybenzoxazines[16,17] has been proposed using cardanol (bio-phenol). Cardanol-based benzoxazine resins are in liquid form due to the presence of a long aliphatic group in the *meta* position. Cardanol-based benzoxazine exhibits good storage stability at room temperature, low heat release, near-zero shrinkage during curing and a low water uptake, which make polybenzoxazines more suitable materials for commercial applications.[6,18–21] Bio-fillers (rice husk ash, palm flower carbon)

from sustainable sources are considered valuable reinforcement for bio-benzoxazines for enhancing their thermal, mechanical and electrical properties to make them suitable for different industrial applications.[22–24] The authors' research group has developed and reported earlier some bio-based polybenzoxazine composites for low-dielectric, oil–water-separation, sound-absorption and corrosion-resistance applications.[25,26]

This investigation focuses on the development of bio-benzoxazine composites from cardanol and a bio-filler (*Aerva lanata* ash (AL-ash)). These composites have improved thermal stability, a good hydrophobic behaviour and enhanced anti-corrosive properties. Cardanol-based bi-functional benzoxazine was developed with cardanol, *p*-phenylenediamine and paraformaldehyde under suitable experimental conditions. The molecular structure was elucidated using the Fourier transform infrared (FTIR) and hydrogen-1 (^{1}H) nuclear magnetic resonance (NMR) spectroscopic techniques. The curing behaviour of bio-benzoxazine was studied using the differential scanning calorimetry (DSC) technique. Further, bio-ash was extracted from the *A. lanata* plant, which contains around 15% ash content, and functionalised with 3-glycidoxypropyltrimethoxysilane (GPTMS). It was used to reinforce cardanol-based 1,4-bis(7-pentadecyl-2*H*-benzo [1,3]oxazin-3(4*H*)-yl)benzene (C-*p*pda) benzoxazine to obtain composites. The thermal stability, morphology and hydrophobic behaviour of the bio-composites were analysed using thermogravimetric analysis (TGA), field emission scanning electron microscopy (FESEM) and goniometry, respectively. The corrosion resistance behaviour was studied using an electrochemical workstation. Data obtained from different studies indicate that the bio-composites developed in this work can be used in the form of insulators, sealants, adhesives, coatings and matrices, the application of which demands a high-temperature and humid environment for different engineering applications.

2. Experimental method

2.1 Materials

Cardanol was obtained from Sathya cashew products (Chennai). Analytical-grade paraformaldehyde was purchased from Sigma-Aldrich, India, and *p*-phenylenediamine was purchased from Alfa Aesar, Mumbai, India. Ethyl acetate was purchased from Thomas Baker, India. Sodium hydroxide (NaOH) and sodium sulfate (Na_2SO_4) were purchased from Merck, Mumbai, India. An *A. lanata* plant was collected from the local area (Coimbatore, India).

2.2 Synthesis of C-*p*pda

About 5 g (0.04 mol) of *p*-phenylenediamine was mixed with 27.6 g (0.08 mol) of cardanol, and 5.5 g (0.16 mol) of paraformaldehyde was added portion-wise in a 100 ml double-necked round-bottomed flask under constant stirring in the absence of any solvent. Then, the temperature was raised to 110°C and maintained for more than 4 h until the completion of formation of benzoxazine. The progress of the reaction was monitored with thin-layer chromatography (8:2 hexane:ethyl acetate solvent). After completion of the reaction, the resinous crude product obtained was dissolved in 50 ml of ethyl acetate and washed twice with 2 N sodium hydroxide for removal of unreacted phenolic compound. Further, the organic layer was washed twice with 100 ml of distilled water. Then, the organic phase was dried over anhydrous sodium sulfate and ethyl acetate was removed using a rotary evaporator to recover the product. The synthesised cardanol-based benzoxazine was labelled as C-*p*pda (Scheme 1).

2.3 Preparation of functionalised AL-ash

The *A. lanata* flowers and leaves were washed repeatedly with distilled water and dried at about 60°C overnight. The dried material was subsequently heated at 600°C for 3 h in a muffle furnace to obtain AL-ash, which predominantly contained calcium oxide, magnesium oxide, iron oxide, phosphorus oxide and silica (SiO_2). The prepared AL-ash (bio-ash) was then functionalised with GPTMS to reinforce benzoxazine. About, 4 ml of GPTMS was stirred with 95% absolute ethanol and 5% deionised water and sonicated for 20 min. Subsequently, 10 g of bio-ash was added, and the resulting mixture was sonicated for another 2 h and then refluxed for 24 h at 80°C. The obtained product was then centrifuged and washed with water followed by ethanol and hexane. The functionalised bio-ash (Scheme 2) was further dried in hot-air oven at 100°C to remove moisture.[27]

2.4 Preparation of polybenzoxazine

Thermal ring-opening polymerisation of cardanol-based benzoxazine was carried out according to a reported procedure (Scheme 3).[28] A typical procedure for polymerisation is as

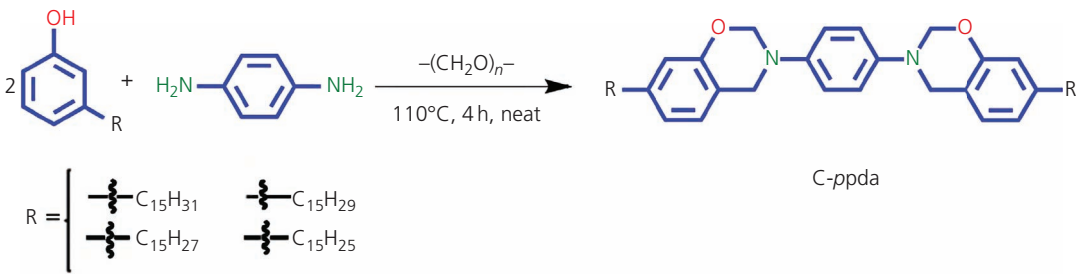

Scheme 1. Synthesis of C-*p*pda

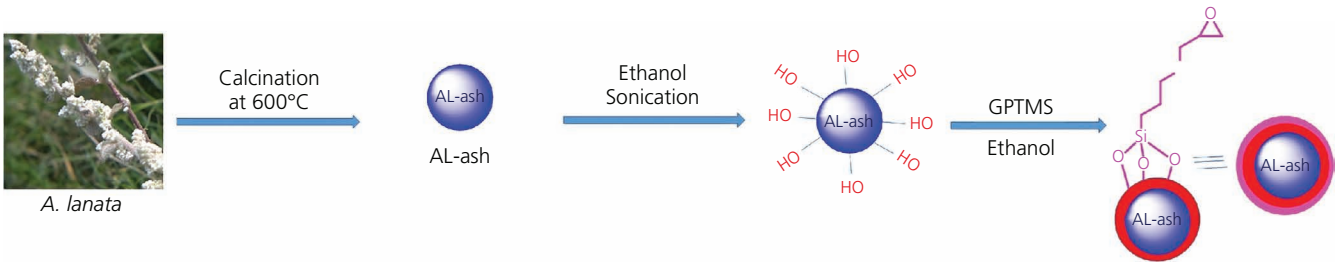

Scheme 2. Preparation of AL-ash and functionalisation with GPTMS

follows: the amine-based homogeneous benzoxazine monomer was placed in the oven at 80°C for 8 h for stabilisation and for removal of moisture and traces of solvent, if any was present. After stabilisation, the temperature was raised to 240°C at a heating rate of 20°C/h. The heating was continued for another 3 h at 240°C for the completion of the curing process. At this temperature, the monomer underwent ring-opening polymerisation to form polybenzoxazine with a cross-linked network structure. The mechanism of polymerisation was confirmed by FTIR spectroscopy.

2.5 Preparation of bio-composites

The formation of AL-ash-reinforced poly(C-*p*pda) is presented in Scheme 4. C-*p*pda was reinforced with 5, 10 and 15 wt% GPTMS-functionalised AL-ash separately and stirred for 1 h to obtain homogeneous blends. The hybrid composites obtained were cured separately in a similar manner as carried out for the preparation of neat matrix.

2.6 Characterisation

FTIR spectral measurements were carried out using a Shimadzu FTIR spectrophotometer. The spectra were recorded in the wave number range 400–4000 cm^{-1}. Hydrogen-1 NMR spectra were obtained with a Bruker spectrometer (400 MHz) using dimethyl sulfoxide-d_6 as a solvent and tetramethylsilane as an internal standard. DSC measurements were recorded using a Netzsch STA 449F3 thermal analyser under a nitrogen (N_2) gas purge (60 ml/min) at a scanning rate of 10°C/min. TGA was carried out from room temperature to 850°C using a Netzsch STA 449F3 thermal analyser with 5 mg of the sample under a nitrogen gas flow (60 ml/min) at a heating rate of 20°C/min. The morphology of the matrix and composites was analysed using an FEI Quanta 200F field emission scanning electron microscope. Energy-dispersive X-ray spectroscopy (EDX) analysis (Hitachi model S-4800), carried out at 20 keV, was used to confirm the percentage elemental composition of AL-ash. Water contact angle measurements were obtained using a Kyowa goniometer with 5 µl of water as probe liquid. Benzoxazine-coated mild steel (MS) plates were tested for corrosion protection behaviour on MS surfaces in 3.5% sodium chloride (NaCl) solution. The corrosion experiments on MS specimens were carried out using open-circuit potential (OCP), electrochemical impedance spectroscopy (EIS) and potentiodynamic polarisation.

3. Results and discussion

Cardanol-based benzoxazine (C-*p*pda) was prepared through the condensation reaction of cardanol with an amino compound and formaldehyde under appropriate reaction conditions as shown in Scheme 1. Due to the presence of *meta*-substituted long alkenes/alkyl (15-carbon) chain groups, the benzoxazine derived from cardanol existed in liquid form. Consequently, the resulting benzoxazine possessed improved flexibility and good water repellence.

3.1 Spectroscopy of cardanol-based benzoxazine

The FTIR spectrum of cardanol-based benzoxazine is presented in Figure 1(a); the results obtained are presented in Table 1. The bands appearing at 1238 and 1096 cm^{-1} were attributed to the asymmetric and symmetric stretching vibrations of the C–O–C bond in benzoxazine, respectively.[29] The peak appearing at

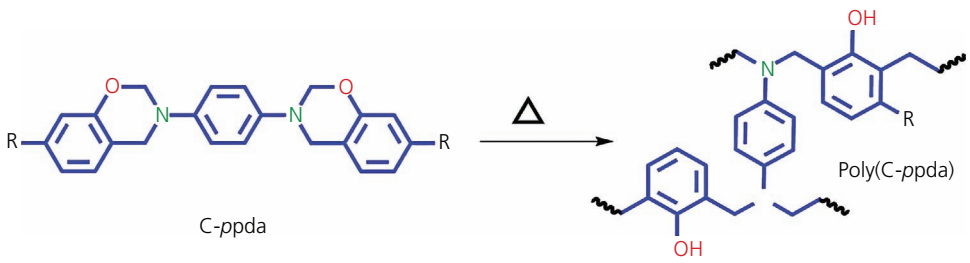

Scheme 3. Ring-opening polymerisation of C-*p*pda

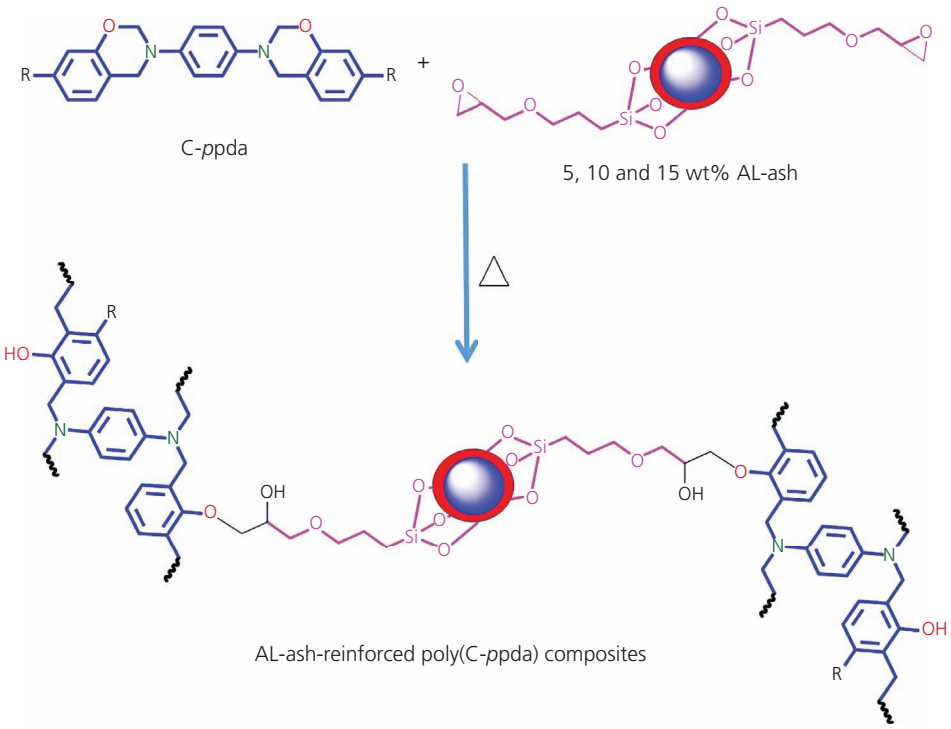

Scheme 4. AL-ash-reinforced polybenzoxazine composites

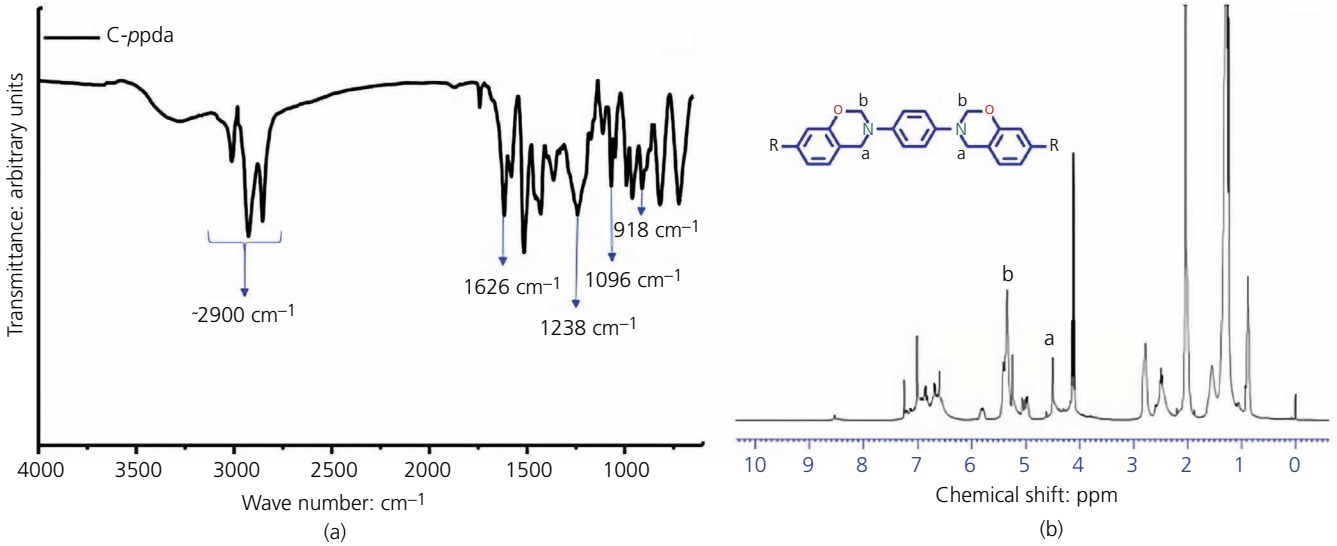

Figure 1. (a) FTIR spectrum of the C-*p*pda benzoxazine monomer; (b) hydrogen-1 NMR spectrum of C-*p*pda benzoxazine. ppm, parts per million

1189 cm^{-1} was obtained due to the asymmetric stretching of C–N–C. Similarly, the appearance of bands around 918 and 1496 cm^{-1} corresponded to a trisubstituted benzene ring, which confirmed the formation of the benzoxazine ring.[29,30] The band appearing around 3009 cm^{-1} corresponded to the C–H stretching vibration of the benzene ring. The characteristic absorption peaks appearing at 2925 and 2853 cm^{-1} represented respectively the asymmetric and symmetric stretching vibrations of the CH_2 of the oxazine ring, as well as the alkyl side chain of the cardanol moiety.[25] Additionally, the structure of the benzoxazine compound was confirmed by hydrogen-1 NMR spectroscopy. The formation of the benzoxazine ring in C-*p*pda was confirmed by

Table 1. FTIR interpretation of the neat polybenzoxazine matrix and AL-ash-reinforced poly(C-*p*pda) composites

Sample	Functional group assignment	Wave number: cm^{-1}	Reference
C-*p*pda	Asymmetric and symmetric stretching vibrations of the C–O–C group	1238 and 1096	Ishida and Agag[29]
	Asymmetric stretching vibration of the C–N–C group	1189	Ishida and Agag[29] and Han *et al.*[30]
	Stretching vibration of the trisubstituted benzene ring	918 and 1496	Ishida and Agag[29] and Han *et al.*[30]
	Stretching vibration of the C–H group	3009	Arumugam *et al.*[25]
	Asymmetric and symmetric stretching vibrations of the CH_2 of the oxazine ring as well as the alkyl side chain of the cardanol moiety	2925 and 2853	Arumugam *et al.*[25]
Poly(C-*p*pda)	–OH of the polybenzoxazine network structure	3360	Sriharshitha *et al.*[31]
Poly(C-*p*pda) composites	Asymmetric stretching and symmetric stretching vibrations of Si–O–Si– linkages	1080 and 820	Han *et al.*[30] and Krishnamoorthy *et al.*[32]

the appearance of resonance peaks at around 4.5 parts per million (ppm) (singlet, 2H, type a signal in Figure 1(b)) for the methylene group of Ar–CH_2–N and around 5.5 ppm (singlet, 2H, type b signal in Figure 1(b)) for O–CH_2–N from hydrogen-1 NMR spectroscopy (Figure 1(b)).

3.2 Curing behaviour of benzoxazine

The curing behaviour of the synthesised neat C-*p*pda benzoxazine monomers, 5, 10 and 15 wt% AL-ash-filled C-*p*pda, was examined by DSC analysis and is shown in Figure 2. The appearance of the exothermic peak of C-*p*pda benzoxazine confirmed that the polymerisation proceeded through a thermal ring-opening mechanism. The curing temperatures (exotherm maxima) of neat C-*p*pda and 5, 10 and 15 wt% AL-ash-reinforced C-*p*pda were observed to be 239, 229, 225 and 223°C (Figure 2(a)), respectively. The curing temperature of benzoxazine reduced with an increasing weight percentage of AL-ash. This migh be the influence of the different types of metal oxides present in AL-ash. In general, the curing temperature of bi-functional benzoxazine was lower than that of mono-functional benzoxazine. The curing temperature of bi-functional benzoxazine obtained from cardanol and diaminodiphenyl amine was observed to be 250°C, which was lower than the curing temperature of mono-functional benzoxazine cardanol–aniline (275°C). Similarly, the curing temperature of C-*p*pda bi-functional benzoxazine was lower than that of cardanol–aniline benzoxazine.[31] In addition, after curing, the samples were checked by DSC analysis, and no exothermic peak was observed (Figure 2(b)), which ascertained the complete polymerisation (curing) of benzoxazine.

3.3 Spectroscopy and thermal behaviour of bio-composites

After the thermal treatment, the chemical structure of cardanol-based polybenzoxazine poly(C-*p*pda) was confirmed from FTIR spectral analysis. The peak appearing at 918 cm^{-1} (O–CH_2–N stretching) indicated the formation of monomeric benzoxazines, and it disappeared after thermal curing at 280°C for 3 h for the samples of poly(C-*p*pda) and AL-ash-reinforced poly(C-*p*pda)

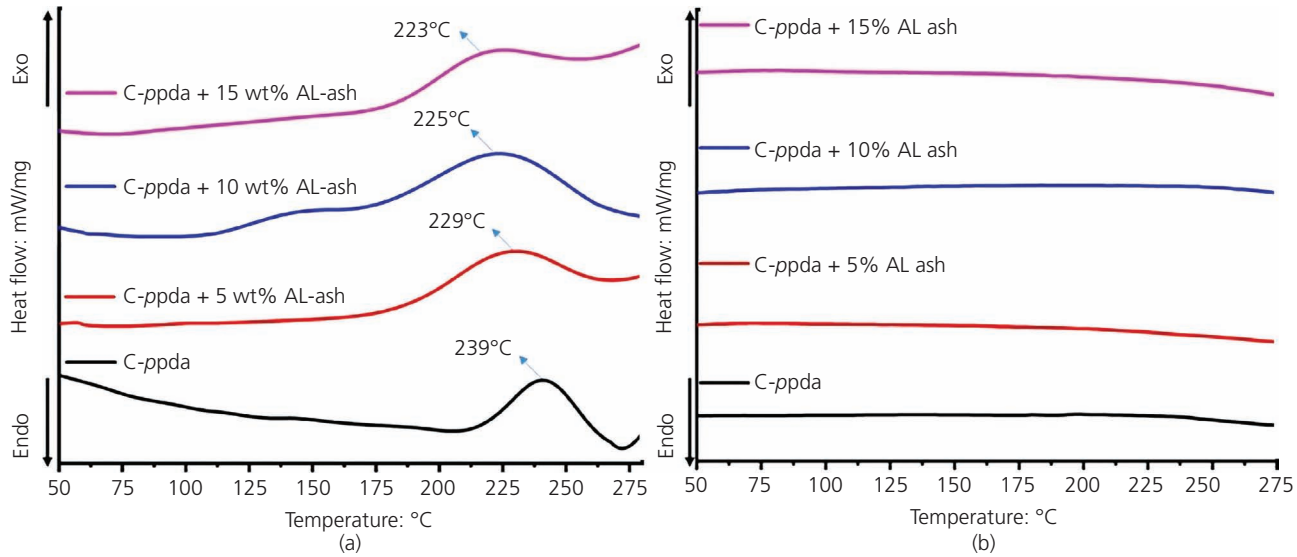

Figure 2. (a) DSC thermograms of AL-ash-reinforced C-*p*pda benzoxazine and (b) DSC thermograms of poly(C-*p*pda) composites

composites (Figure 3), which confirms the occurrence of complete ring opening and the formation of a three-dimensional cross-linking network structure through polymerisation of the benzoxazine monomer. The broad peak appearing at 3360 cm^{-1} confirms the –OH of the polybenzoxazine network structure.[31] The peaks appearing at 1080 and 820 cm^{-1} indicate the presence of Si–O–Si– linkages of asymmetric stretching and symmetric stretching vibration,[30,32] respectively (Table 1) for the AL-ash-reinforced polybenzoxazine composites.

The thermal degradation behaviour of the cardanol-based benzoxazine poly(C-*p*pda) and GPTMS-functionalised AL-ash-reinforced poly(C-*p*pda) composites was analysed by TGA (Figure 4), and the results obtained are presented in Table 2. The thermal stability of the polybenzoxazine matrix was one of the important factors to consider in device fabrication to predict the thermal resistance and flame-retardant behaviour. TGA provided valuable data with regard to the thermal stability of materials, the number of impurities or solvents present and the nature of degradation, which was done by measuring the weight loss at each instant. For cardanol-based benzoxazine poly (C-*p*pda), a 5% weight loss was observed at 335°C. The maximum degradation took place at 441°C. The percentage char yield of the samples was obtained at 850°C from Figure 4. A 23% residual char yield was observed for the poly(C-*p*pda) benzoxazine matrix. Poly(C-*p*pda) had a higher char yield than cardanol–aniline-based polybenzoxazine (poly(C-a)), due to the formation of a higher cross-linked network structure contributed by the bi-functional benzoxazine moiety.[29]

The values of temperature required for 5% ($T_{d5\%}$) weight loss for the neat matrix and 5, 10 and 15 wt% AL-ash-reinforced poly(C-*p*pda) composites were found to be 335, 336, 340 and 341°C, respectively.

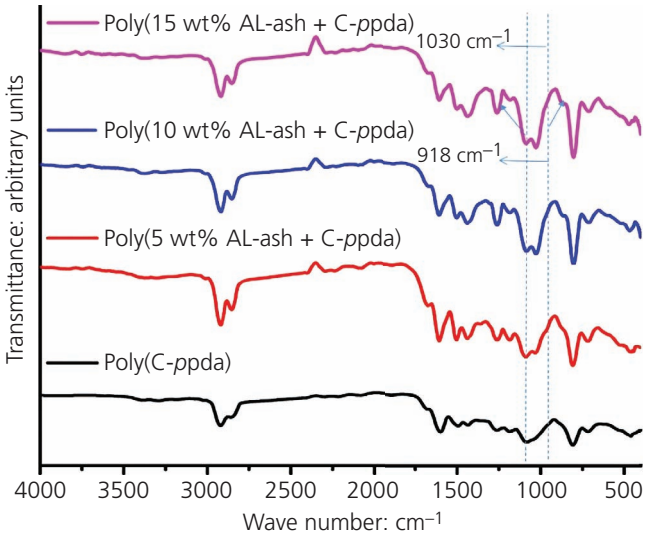

Figure 3. FTIR spectra of AL-ash-reinforced poly(C-*p*pda) composites

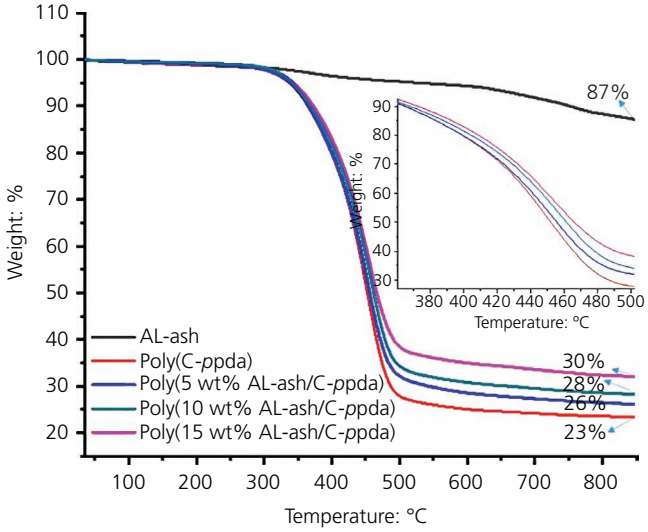

Figure 4. TGA thermograms of AL-ash-reinforced poly(C-*p*pda) composites

Similarly, the maximum degradation temperatures (T_{dmax}) obtained for the AL-ash-reinforced poly(C-*p*pda) composites were 445, 448 and 452°C, respectively. The thermal stability and char yields of AL-ash-reinforced poly(C-*p*pda) composites were found to gradually increase with an increased weight percentage incorporation of the reinforcement (Table 2). The char yields of 5, 10 and 15 wt% AL-ash-reinforced poly(C-*p*pda) composite systems were found to be 28, 29 and 32%, respectively. In addition, it was observed when the TGA results were compared with DSC results, the polymerisation temperature (curing) decreased, with an increase in thermal stability with increasing percentage incorporation of AL-ash.

3.4 Flame-retardant behaviour

Polymers having a better flame-retardant behaviour play key roles in different engineering applications, where high flame retardance and thermal stability are required. Flame retardants are generally classified based on their chemical composition, grouped by whether they contain bromine, chlorine, phosphorus, nitrogen, boron or mineral fillers. Polybenzoxazine is a nitrogen-rich polymer that enhances the flame-retardant behaviour. AL-ash also contains a silica network and metal oxide, which in turn promote the flame-retardant behaviour. The flame-retardant behaviour of the cured benzoxazine matrix is ascertained by using the value of residual char yield obtained from TGA at 850°C. The value of the limiting oxygen index (LOI) is calculated from the van Krevelen and Hoftyzer equation (Equation 1),[33–36] and the results obtained are presented in Table 2.

$$\text{LOI} = 17.5 + 0.4(\theta) \quad (1)$$

where θ is the percentage char yield of materials at 850°C.

Table 2. Thermal behaviour of the neat polybenzoxazine matrix and AL-ash-reinforced poly(C-*p*pda) composites

Sample	5% weight loss: °C	10% weight loss: °C	T_{dmax}: °C	Char yield at 850°C: %	LOI
AL-ash	520	751	755	87	52
Poly(C-*p*pda)	335	361	441	23	27
5 wt% AL-ash + poly(C-*p*pda)	336	365	445	26	28
10 wt% AL-ash + poly(C-*p*pda)	340	366	448	28	29
15 wt% AL-ash + poly(C-*p*pda)	341	370	452	33	32

LOI, limiting oxygen index

The char yield of the polybenzoxazine matrix, poly(C-*p*pda), is found to be in the range of about 20%. The LOI values of the polymers should be above the threshold value of 26 to render them self-extinguishing and for suitability for many applications requiring good flame resistance. The synthesised polybenzoxazine shows an LOI value close to 26, confirming its good flame-retardant properties. The obtained LOI value of poly(C-*p*pda) is 25. This indicates that poly(C-*p*pda) has a higher LOI value than mono-functional poly(C-a), due to the formation of a higher cross-linked network.[23,33] The LOIs of AL-ash-reinforced poly(C-*p*pda) composites were found to gradually increase with an increased weight percentage incorporation of reinforcement (Table 2). The LOI values of 5, 10 and 15 wt% AL-ash-reinforced poly(C-*p*pda) composites were found to be 28, 29 and 32%, respectively.

3.5 Morphology

FESEM images of the AL-ash-reinforced poly(C-*p*pda) composites are shown in Figure 5. Figures 5(a) and 5(b) show the FESEM images of AL-ash particles. The EDX spectra in Figure 6(a) show the elements present in AL-ash – namely, oxygen (40%), calcium (9%), magnesium (6%), iron (1%), phosphorus (2%), silicon (5%) and potassium (13%) – which help enhance thermal stability and corrosion resistance behaviour. The 15 wt% AL-ash-reinforced poly(C-*p*pda) composite material was taken as a representative sample for FESEM (Figure 5) and EDX

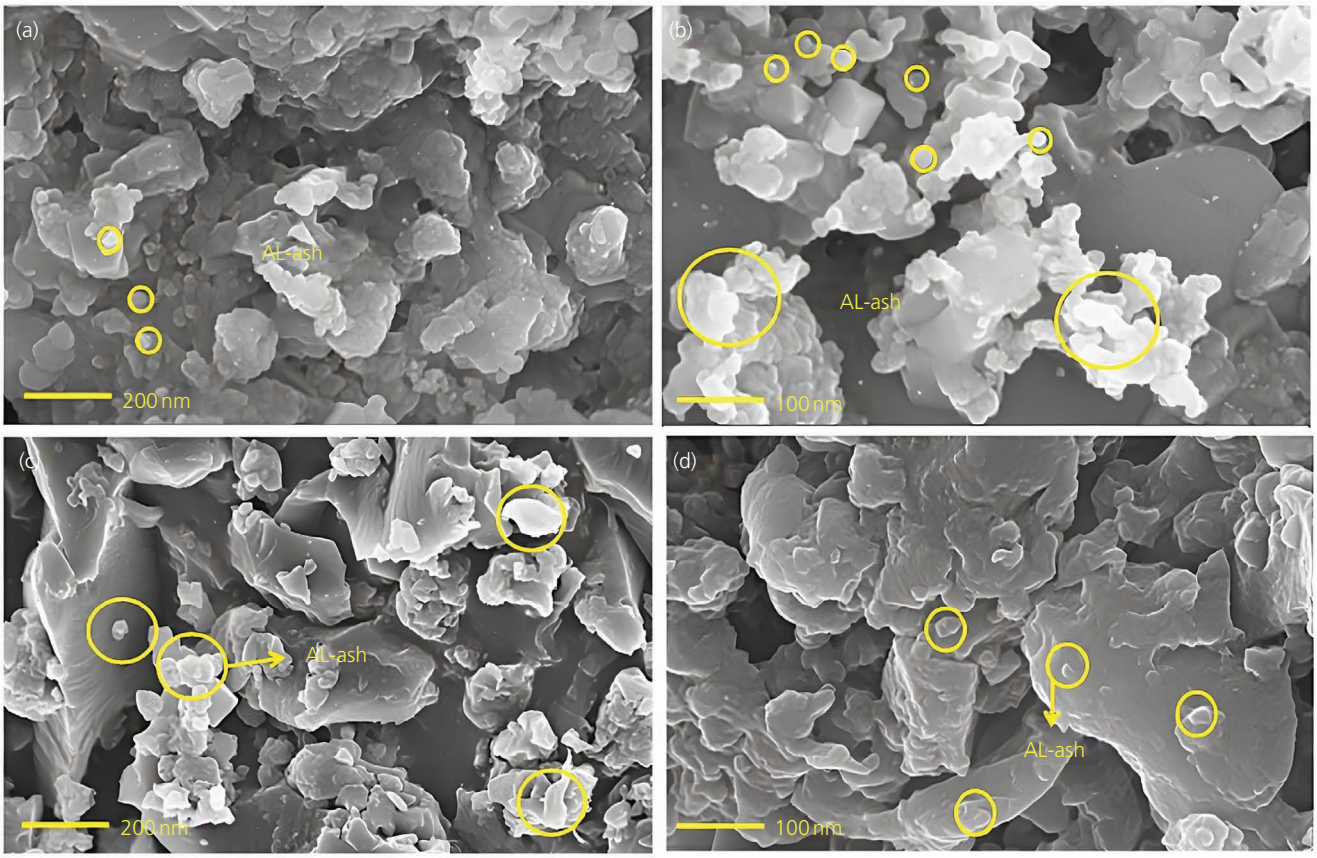

Figure 5. FESEM images of (a, b) AL-ash and (c, d) AL-silica-reinforced poly(C-*p*pda) composites

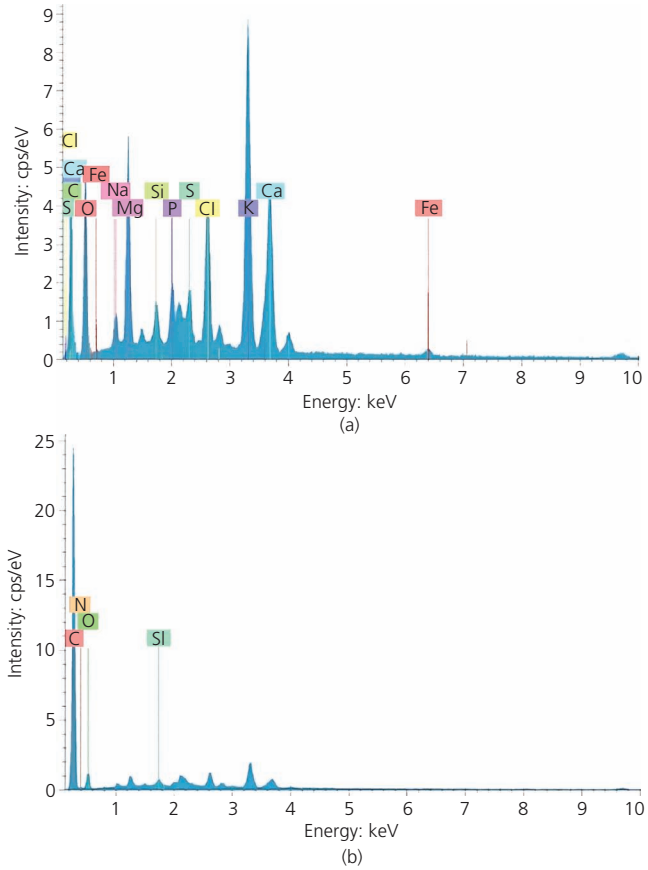

Figure 6. EDX spectra of (a) AL-ash and (b) AL-ash-reinforced poly (C-*p*pda) composites. cps, counts per second

analysis (Figure 6). The AL-ash-reinforced poly(C-*p*pda) composite possessed a homogenous morphology, and AL-ash was dispersed uniformly and in turn provided composites without any cracking and voids and thus contributed to improved thermal properties.

3.6 Water contact angle

The values of the water contact angles of neat poly(C-*p*pda) and AL-ash-reinforced poly(C-*p*pda) composites were observed to be around 148 ± 2°. Figure 7 presents the water contact angle images of neat polybenzoxazine (poly(C-*p*pda)) and the AL-ash-reinforced poly(C-*p*pda) composites. The lower affinity of the developed polybenzoxazine matrix indicates its inherent hydrophobic behaviour. This behaviour mainly arises due to the *meta*-substituted long aliphatic chain of the cardanol moiety. The value of water contact angle obtained is compared with previously reported values for cardanol-based benzoxazines.[33] All values of the water contact angles of cardanol-based benzoxazine reach more than 148°. The 15 wt% AL-ash-loaded poly(C-*p*pda) composite possesses a higher value of water contact angle than neat polybenzoxazine and other AL-ash-reinforced poly(C-*p*pda) composites.

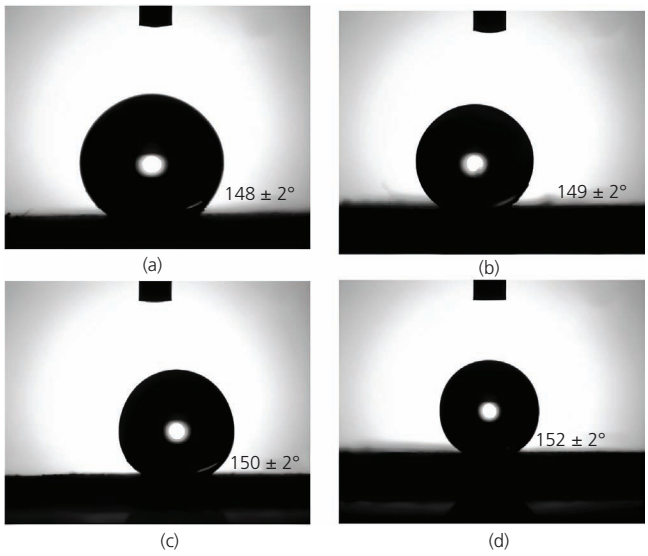

Figure 7. Water contact angle images of (a) poly(C-*p*pda), (b) poly (5 wt% AL-ash/C-*p*pda) (c) poly(10 wt% AL-ash/C-*p*pda) and (d) poly(15 wt% AL-ash/C-*p*pda)

3.7 Corrosion resistance

The corrosion protection efficiency of MS specimens coated with the cardanol-derived benzoxazines and AL-ash-reinforced composites in 3.5% sodium chloride solution was studied using OCP, EIS and potentiodynamic polarisation. Among the polybenzoxazine-composite-coated MS specimens, those coated with 15 wt% AL-ash-reinforced polybenzoxazine composite coatings exhibited better protection of MS against corrosion.

EIS was used to assess the corrosion resistance behaviour of neat polybenzoxazine, poly(C-*p*pda) and AL-ash-reinforced poly(C-*p*pda) composite coatings on MS. Impedance analysis was performed using MS plates with a 2 cm^2 area. After coating, the specimens were immersed in 3.5% sodium chloride solution for different time periods. The OCP values were measured. It can be understood from the values of OCP that the coated specimens shifted significantly to the anodic direction when compared with the bare MS specimen. It can also be seen that the OCP values of the specimens coated with neat polybenzoxazine (poly(C-*p*pda)) and AL-ash-reinforced poly(C-*p*pda) composites decreased at a much slower rate when compared with that of the bare MS specimen. The OCP shifting to increasingly positive values indicated the high corrosion resistance of the coatings.[37–39] Among the specimens coated with the neat polybenzoxazine matrix and AL-ash-reinforced polybenzoxazine composites, the specimen coated with poly(C-*p*pda) with 15 wt% AL-ash shows a higher anodic shift of OCP values, which indicates that this sample is less porous and forms a better adherent film on the surface of MS than the other specimens, which reduces the permeability of the corrosion medium into the film, thus providing higher corrosion protection.[40,41]

Nyquist plots were derived from the EIS measurements for five different MS specimens coated with neat polybenzoxazines and varying weight percentages of AL-ash-reinforced polybenzoxazine composites and uncoated MS specimens after immersion in 3.5% sodium chloride solution for 5 days. The results obtained are presented in Figure 8. The uncoated MS specimen exhibits a small capacitive loop, indicating its poor corrosion-resistance behaviour, whereas specimens coated with neat poly(C-*p*pda) and AL-ash-reinforced poly(C-*p*pda) possess a single capacitive loop. The EIS data obtained are fitted using the equivalent circuit model in Figure 9 for comparison.

The equivalent circuit was used to evaluate the data, where R_s is the solution resistance of the solution between the working electrode and the counter electrode. R_s values not only depend on the ionic conductivity of the solution but also depend on the geometrical area of the electrode. R_s values are not important data in studying the corrosion behaviour of the film because they do not yield any information about the coatings. R_{ct} is the charge-transfer resistance, which is used to measure the resistance of the electron transfer across the metal–solution interface, which is inversely proportional to the corrosion rate (CR) of the metal.

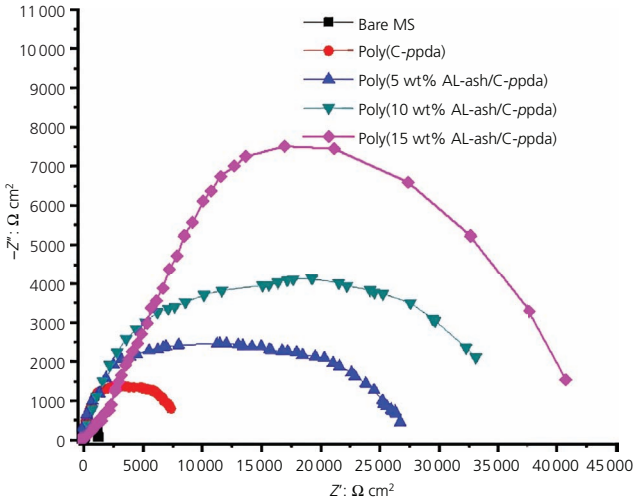

Figure 8. EIS responses of bare MS specimen and specimens coated with neat polybenzoxazine and AL-ash-reinforced polybenzoxazine composites in 3.5% sodium chloride solution

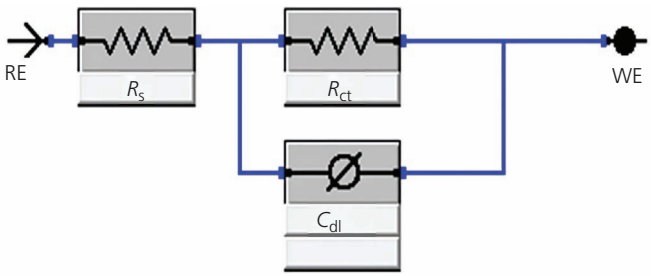

Figure 9. Electrical circuit model used to fit EIS results. RE, reference electrode; WE, working electrode

R_c is the coating resistance, and C_{dl} is the coating capacitance. The calculated values of the corrosion parameters from EIS measurements are presented in Table 3. The R_{ct} values of the AL-ash-reinforced polybenzoxazine-coated specimens are higher than that of the bare MS. Corrosion resistance also increases when a higher percentage of AL-ash is incorporated into the polybenzoxazine matrix. Maximum R_c and R_{ct} values are obtained for the MS specimen coated with polybenzoxazine with 15 wt% AL-ash. The improved corrosion resistance observed may be due to the reduction of pores/cavities present in the polybenzoxazine coating rich in AL-ash.[38,42,43] The roughness factor values (n) continuously decrease with an increasing concentration of AL-ash into the polybenzoxazine matrix, which also corresponds to the reduction of pores/cavities on the coated MS surface. Generally, all the organic coatings are not completely impenetrable for long time; their barrier properties could weaken when the immersion time increases because of water/corrosion medium penetration into the coatings. For bare MS, the corrosion medium has direct contact with the metal surface, which leads to the generation of many electroactive sites and the corrosion process starts slowly. Actually, a corrosion reaction will take place in the presence of moisture and oxygen.

AL-ash-containing polybenzoxazine coatings prevent the diffusion of oxygen and aggressive medium into the coatings due to the highly cross-linked network structure of the polybenzoxazine matrix and AL-ash-reinforced composite coatings. From the water contact angle measurements, it can also be understood that all the samples of AL-ash-reinforced polybenzoxazine composites are hydrophobic in nature, which could effectively reduce the wettability of polymer coatings and in turn ultimately reduce the sorption of water molecules by the coatings. Among the different coating samples used in the present work – namely, neat polybenzoxazine matrix and AL-ash-reinforced polybenzoxazines – poly(C-*p*pda) with 15 wt% AL-ash offers better corrosion protection to the MS surface than the other samples due to efficient interaction with the metal surface, which in turn forms a strong and firm adherent film resisting the penetration of water molecules.

Figure 10 shows the Tafel plots of MS specimens coated with poly(C-*p*pda) and AL-ash-reinforced poly(C-*p*pda). The CR was calculated using I_{corr} values using the following equation:

$$2.\quad \mathrm{CR} = MI_{corr}/\rho nF$$

where M was the molecular mass of copper (55.85 g/mol); I_{corr} was the corrosion current density (A/cm^2); F was the Faraday constant (96 500 A/mol); ρ was the density of the MS specimen

Table 3. Values of corrosion parameters calculated from potentiodynamic polarisation studies for the coated and bare MS specimens in 3.5% sodium chloride solution

Sample	R_s: Ω cm^2	R_{ct}: Ω cm^2	$Y_{0,dl}$: μs^n/(Ω cm^2)	n_{dl}	C_{dl}: μF/cm^2
Bare steel specimen	12	1.24×10^3	87.82	0.87	59.8
Poly(C-*p*pda)	24	8.21×10^3	3.91	0.75	0.6
5 wt% AL-ash + poly(C-*p*pda)	67	2.75×10^4	3.10	0.81	1.1
10 wt% AL-ash + poly(C-*p*pda)	81	3.62×10^4	2.41	0.83	1.8
15 wt% AL-ash + poly(C-*p*pda)	39	4.24×10^4	0.12	0.27	0.8

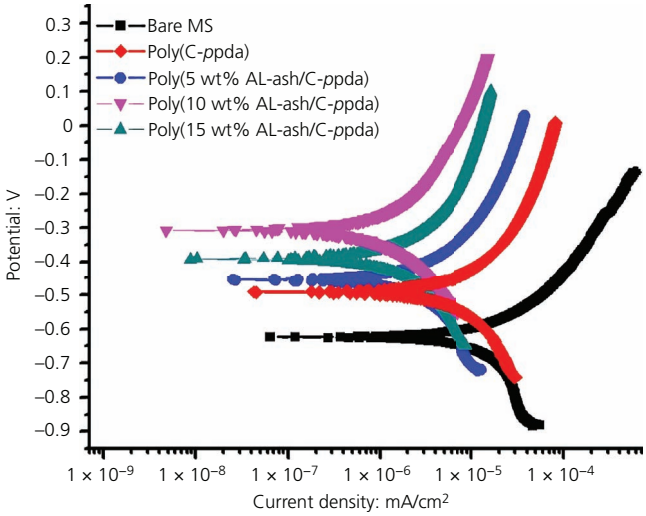

Figure 10. Tafel plots of bare MS specimen and specimens coated with neat polybenzoxazine matrix and AL-ash-reinforced polybenzoxazine composites in 3.5% sodium chloride solution

(7.85 g/cm^3); and n was the number of electrons transferred during corrosion reaction, which was assumed to be 2.

It was observed from the studies that the E_{corr} values of the specimens coated with AL-ash-reinforced poly(C-*p*pda) shifted anodically and a higher anodic shift was observed for specimens coated with AL-ash-reinforced polybenzoxazine. The maximum anodic shift was observed for the MS specimen coated with 15 wt% AL-ash-reinforced poly(*p*pda). The I_{corr} values of the specimens coated with AL-ash-reinforced poly(*p*pda) were also lower, which indicated the better corrosion resistance of the coated specimens (Table 4). These results corresponded to the data observed in the EIS. The improved corrosion resistance might be due to the incorporation of AL-ash into polybenzoxazine, which suppressed the anodic corrosion reactions.[43]

Among the composites, the 15 wt% AL-ash-loaded poly(C-*p*pda) coating offered better corrosion protection to MS specimens than the other samples of coatings studied in the present work. The resulting AL-ash-reinforced poly(C-*p*pda) showed better performance than previously reported cardanol-based benzoxazines.[44,45] The anti-corrosion efficiencies of 40% silane-modified cardanol–triethylenetetramine polybenzoxazine[26] and silica 7 wt% rice husk ash silica-reinforced cardanol–furfuryl polybenzoxazine[27] were 82 and 75%, respectively. It was ascertained from the present work that the corrosion resistance efficiency of 15 wt% AL-ash-reinforced poly(C-*p*pda) was about 95% (Table 4). From the results, it can be concluded that the AL-ash-reinforced poly(C-*p*pda) hybrid composites are suitable for protecting the surfaces of MS specimens from corrosion.

4. Conclusion

Bio-based bi-functional benzoxazine (C-*p*pda) was synthesised using cardanol, *p*-phenylenediamine and paraformaldehyde through solventless Mannich condensation. The benzoxazine monomer obtained was reinforced with varying weight percentages (5, 10 and 15 wt%) of AL-ash derived from *A. lanata* to obtain hybrid composites. Among the AL-ash-reinforced hybrid composites, 15 wt% AL-ash-loaded poly(C-*p*pda) possessed excellent thermal stability as well as a hydrophobic behaviour close to being superhydrophobic. From the corrosion study data, it was inferred that the MS specimens coated with the bio-based benzoxazine matrix and AL-ash-reinforced benzoxazine composites exhibited excellent resistance to corrosion.

Acknowledgements

The authors thank the PSG management, secretary and principal of the PSG Institute of Technology and Applied Research, Coimbatore, India, for their moral and financial support.

Table 4. Corrosion parameters calculated from Tafel studies for the coated and uncoated MS specimens in 3.5% sodium chloride solution

Sample	E_{corr}: mV	I_{corr}: mA	CR: mils/year	β_c: mV/decade	β_a: mV/decade	Efficiency: %
Bare MS	−624	1.61×10^{-5}	6.22×10^{-10}	148.38	94.41	0
Poly(C-*p*pda)	−494	3.90×10^{-6}	1.51×10^{-10}	101.11	101.10	75.6
5 wt% AL-ash + poly(C-*p*pda)	−455	1.75×10^{-6}	6.62×10^{-11}	169.96	105.26	89.4
10 wt% AL-ash + poly(C-*p*pda)	−388	1.25×10^{-6}	4.86×10^{-11}	120.29	106.53	92.2
15 wt% AL-ash + poly(C-*p*pda)	−312	7.6×10^{-7}	2.95×10^{-11}	122.91	107.35	95.3

REFERENCES

1. Ning X and Ishida H (1994) Phenolic materials via ring-opening polymerization: synthesis and characterization of bisphenol-A based benzoxazines and their polymers. *Journal of Polymer Science Part A: Polymer Chemistry* **32(6)**: 1121–1129, https://doi.org/10.1002/pola.1994.080320614.
2. Zhang C, Zhang Y, Zhou Q, Ling H and Gu Y (2014) Processability and mechanical properties of bisbenzoxazine modified by the cardanol-based aromatic diamine benzoxazine. *Journal of Polymer Engineering* **34(6)**: 561–568, https://doi.org/10.1515/polyeng-2014-0018.
3. Krishnadevi K, Selvaraj V and Prasanna D (2015) Thermal, mechanical and antibacterial properties of cyclophosphazene incorporated benzoxazine blended bismaleimide composites. *RSC Advances* **5(2)**: 913–921, https://doi.org/10.1039/C4RA10564H.
4. Zhang X, Liu L, Yu Y and Weng L (2018) Flame-retardant mechanism of benzoxazine resin with triazine structure. *Advances in Polymer Technology* **37(2)**: 384–389, https://doi.org/10.1002/ADV.21677.
5. Chozhan CK, Chandramohan A and Alagar M (2013) Studies on thermal, mechanical, electrical, and morphological behavior of organoclay-reinforced polybenzoxazine–epoxy nanocomposites. *High Performance Polymers* **25(8)**: 1007–1021, https://doi.org/10.1177/0954008313493345.
6. Arumugam H, Krishnan S, Chavali M and Muthukaruppan A (2018) Cardanol based benzoxazine blends and bio-silica reinforced composites: thermal and dielectric properties. *New Journal of Chemistry* **42(6)**: 4067–4080, https://doi.org/10.1039/C7NJ04506A.
7. Krishnan S, Arumugam H, Chavali M and Muthukaruppan A (2019) High dielectric, low curing with high thermally stable renewable eugenol-based polybenzoxazine matrices and nanocomposites. *Journal of Applied Polymer Science* **136(6)**: article 47050, https://doi.org/10.1002/app.47050.
8. Revathi R, Prabunathan P, Kumar M and Alagar M (2016) Studies on graphene oxide-reinforced polybenzoxazine nanocomposites. *High Performance Polymers* **28(4)**: 425–435, https://doi.org/10.1177/0954008315585013.
9. Selvaraj V, Jayanthi KP and Alagar M (2019) Livestock chicken feather fiber reinforced cardanol benzoxazine–epoxy composites for low dielectric and microbial corrosion resistant applications. *Polymer Composites* **40(10)**: 4142–4153, https://doi.org/10.1002/pc.25275.
10. Froimowicz P, Arza CR, Han L and Ishida H (2016) Smart, sustainable, and ecofriendly chemical design of fully bio-based thermally stable thermosets based on benzoxazine chemistry. *ChemSusChem* **9(15)**: 1921–1928, https://doi.org/10.1002/cssc.201600577.
11. Hariharan A, Srinivasan K, Murthy C and Alagar M (2018) Synthesis and characterization of a novel class of low temperature cure benzoxazines. *Journal of Polymer Research* **25(1)**: article 20, https://doi.org/10.1007/s10965-017-1423-0.
12. Lee SH, Kim KS, Shim JH and Ahn CH (2018) High-performance printed circuit board materials based on benzoxazine and epoxy blend system. *Macromolecular Research* **26(4)**: 388–393, https://doi.org/10.1007/s13233-018-6046-7.
13. Hariharan A, Srinivasan K, Murthy C and Alagar M (2017) A novel imidazole-core-based benzoxazine and its blends for high-performance applications. *Industrial & Engineering Chemistry Research* **56(33)**: 9347–9354, https://doi.org/10.1021/acs.iecr.7b01816.
14. Zhang K, Cai R, Zhuang Q *et al.* (2014) High performance crosslinked system based on reaction of benzoxazine with benzoxazole. *Journal of Polymer Science Part A: Polymer Chemistry* **52(11)**: 1514–1518, https://doi.org/10.1002/pola.27153.
15. Baqar M, Agag T, Ishida H and Qutubuddin S (2012) Methylol-functional benzoxazines as precursors for high-performance thermoset polymers: unique simultaneous addition and condensation polymerization behavior. *Journal of Polymer Science Part A: Polymer Chemistry* **50(11)**: 2275–2285, https://doi.org/10.1002/pola.26008.
16. Zhan Z, Yan H, Yin P, Cheng J and Fang Z (2020) Synthesis and properties of a novel bio-based benzoxazine resin with excellent low-temperature curing ability. *Polymer International* **69(4)**: 355–362, https://doi.org/10.1002/pi.5957.
17. Arumugam H, Mohamed Ismail AA, Govindraj L and Muthukaruppan A (2021) Development of bio-based benzoxazines coated melamine foam for oil–water separation. *Progress in Organic Coatings* **153**: article 106128, https://doi.org/10.1016/j.porgcoat.2020.106128.
18. Kurinchyselvan S, Chandramohan A, Hariharan A, Gomathipriya P and Alagar M (2020) Cardanol-based benzoxazine-terminated graphene oxide-reinforced fluorinated benzoxazine hybrid composites for low *K* applications. *Composite Interfaces* **27(8)**: 737–751, https://doi.org/10.1080/09276440.2019.1697132.
19. Vasapollo G, Mele G and Del Sole R (2011) Cardanol-based materials as natural precursors for olefin metathesis. *Molecules* **16(8)**: 6871–6882, https://doi.org/10.3390/molecules16086871.
20. Lochab B, Varma IK and Bijwe J (2012) Cardanol-based bisbenzoxazines: effect of structure on thermal behaviour. *Journal of Thermal Analysis and Calorimetry* **107(2)**: 661–668, https://doi.org/10.1007/s10973-011-1854-5.
21. Shukla S, Yadav N and Lochab B (2017) Cardanol-based benzoxazines and their applications. In *Advanced and Emerging Polybenzoxazine Science and Technology* (Ishida H and Froimowicz P (eds)). Elsevier, Amsterdam, the Netherlands, pp. 451–472.
22. Selvaraj V, Jayanthi KP and Alagar M (2018) Development of biocomposites from agro wastes for low dielectric applications. *Journal of Polymers and the Environment* **26(9)**: 3655–3669, https://doi.org/10.1007/S10924-018-1211-X.
23. Hariharan A, Prabunathan P, Subramanian SS, Kumaravel M and Alagar M (2020) Blends of chalcone benzoxazine and bio-benzoxazines coated cotton fabrics for oil–water separation and bio-silica reinforced nanocomposites for low-*k* applications. *Journal of Polymers and the Environment* **28(2)**: 598–613, https://doi.org/10.1007/s10924-019-01629-2.
24. Selvaraj V, Raghavarshini TR and Alagar M (2020) Development and characterization of palm flower carbon reinforced DOPO–urea diamine based cardanol benzoxazine–epoxy hybrid composites. *Polymer Engineering & Science* **60(4)**: 732–739, https://doi.org/10.1002/pen.25331.
25. Arumugam H, Krishnasamy B, Perumal G *et al.* (2021) Bio-composites of rice husk and saw dust reinforced bio-benzoxazine/epoxy hybridized matrices: thermal, mechanical, electrical resistance and acoustic absorption properties. *Construction and Building Materials* **312**: article 125381, https://doi.org/10.1016/j.conbuildmat.2021.125381.
26. Hariharan A, Prabunathan P, Kumaravel A, Manoj M and Alagar M (2020) Bio-based polybenzoxazine composites for oil–water separation, sound absorption and corrosion resistance applications. *Polymer Testing* **86**: article 106443, https://doi.org/10.1016/j.polymertesting.2020.106443.
27. Krishnadevi K, Devaraju S, Sriharshitha S, Alagar M and Keerthi Priya Y (2020) Environmentally sustainable rice husk ash reinforced cardanol based polybenzoxazine bio-composites for insulation applications. *Polymer Bulletin* **77(5)**: 2501–2520, https://doi.org/10.1007/s00289-019-02854-4.
28. Muthukaruppan A, Arumugam H, Krishnan S, Kannan K and Chavali M (2018) A low cure thermo active polymerization of chalcone based benzoxazine and cross linkable olefin blends. *Journal of Polymer Research* **25(8)**: 163–173, https://doi.org/10.1007/s10965-018-1556-9.
29. Ishida H and Agag T (2011) Overview and historical background of polybenzoxazine research. In *In Handbook of Benzoxazine Resins* (Ishida H and Agag T (eds)). Elsevier, Amsterdam, the Netherlands, pp. 3–81.

30. Han L, Iguchi D, Gil P *et al.* (2017) Oxazine ring-related vibrational modes of benzoxazine monomers using fully aromatically substituted, deuterated, ^{15}N isotope exchanged, and oxazine-ring-substituted compounds and theoretical calculations. *Journal of Physical Chemistry A* **121(33)**: 6269–6282, https://doi.org/10.1021/acs.jpca.7b05249.
31. Sriharshitha S, Krishnadevi K, Devaraju S, Srinivasadesikan V and Lee SL (2020) Eco-friendly sustainable poly(benzoxazine-*co*-urethane) with room-temperature-assisted self-healing based on supramolecular interactions. *ACS Omega* **5(51)**: 33178–33185, https://doi.org/10.1021/acsomega.0c04840.
32. Krishnamoorthy K, Subramani D, Eeda N and Muthukaruppan A (2019) Development and characterization of fully bio-based polybenzoxazine–silica hybrid composites for low-*k* and flame-retardant applications. *Polymers for Advanced Technologies* **30(7)**: 1856–1864, https://doi.org/10.1002/pat.4618.
33. Aishwarya D, Balaji K, Hariharan A, Latha G and Alagar M (2021) Effective low temperature cure cardanol based mono-functional benzoxazines: a comparison. *Polymer Science, Series B* **63(6)**: 727–736, https://doi.org/10.1134/S1560090421060014.
34. Hariharan A, Kesava M, Alagar M, Dinakaran K and Subramanian K (2018) Optical, electrochemical, and thermal behavior of polybenzoxazine copolymers incorporated with tetraphenylimidazole and diphenylquinoline. *Polymers for Advanced Technologies* **29(1)**: 355–363, https://doi.org/10.1002/pat.4122.
35. Van Krevelen DW (1997) Cohesive properties and solubility. In *Properties of Polymers: Their Correlation with Chemical Structure; Their Numerical Estimation and Prediction from Additive Group Contributions*, 3rd edn. Elsevier Amsterdam, the Netherlands, pp. 189–225.
36. Van Krevelen DW and Hoftyzer PJ (1976) *Properties of Polymers, Their Estimation and Correlation with Chemical Structure*, 2nd edn. Elsevier Scientific Publishing, Amsterdam, the Netherlands.
37. Muthusamy M, Balaji K, Murugavel SC, Yuan C and Dai L (2020) Synthesis and characterization of liquid crystalline polyesters containing α,β-unsaturated ketone moiety in the main chain derived from 2,6-bis(4-hydroxybenzylidene) cyclohexanone. *Polymer Science Series B* **62(3)**: 245–255, https://doi.org/10.1134/S1560090420030112.
38. Khodair ZT, Khadom AA and Jasim HA (2018) Corrosion protection of mild steel in different aqueous media via epoxy/nanomaterial coating: preparation, characterization and mathematical views. *Integrative Medicine Research* **12(1)**: 424–435, https://doi.org/10.1016/j.jmrt.2018.03.003.
39. Zhou C, Lu X, Xin Z, Liu J and Zhang Y (2014) Polybenzoxazine/SiO_2 nanocomposite coatings for corrosion protection of mild steel. *Corrosion Science* **80**: 269–275, https://doi.org/10.1016/j.corsci.2013.11.042.
40. Zhou C, Lu X, Xin Z and Liu (2013) Corrosion resistance of novel silane-functional polybenzoxazine coating on steel. *Corrosion Science* **70**: 145–151, https://doi.org/10.1016/j.corsci.2013.01.023.
41. Behzadnasab M, Mirabedini SM, Kabiri K and Jamali S (2011) Corrosion performance of epoxy coatings containing silane treated ZrO_2 nanoparticles on mild steel in 3.5% NaCl solution. *Corrosion Science* **53(1)**: 89–98, https://doi.org/10.1016/j.corsci.2010.09.026.
42. Rekha MY and Srivastava C (2019) Microstructure and corrosion properties of zinc–graphene oxide composite coatings. *Corrosion Science* **152**: 234–248, https://doi.org/10.1016/j.corsci.2019.03.015.
43. Atuanya CU, Ekweghiariri DI and Obele CM (2018) Experimental study on the microstructural and anti-corrosion behaviour of Co-deposition Ni–Co–SiO_2 composite coating on mild steel. *Defence Technology* **14(1)**: 64–69, https://doi.org/10.1016/j.dt.2017.10.001.
44. Derradji M, Ramdani N and Zhang T (2016) Effect of silane surface modified titania nanoparticles on the thermal, mechanical, and corrosion protective properties of a bisphenol-A based phthalonitrile resin. *Progress in Organic Coatings* **90**: 34–43, https://doi.org/10.1016/j.porgcoat.2015.09.021.
45. Lakshmikandhan T, Hariharan A, Sethuraman K and Alagar M (2019) Development of functionalized SiO_2–TiO_2 reinforced cardanol and caprolactam modified diamine based polybenzoxazine nanocomposites for high performance applications. *Journal of Coatings Technology and Research* **16(6)**: 1737–1749, https://doi.org/10.1007/s11998-019-00263-w.

How can you contribute?

To discuss this paper, please submit up to 500 words to the journal office at support@emerald.com. Your contribution will be forwarded to the author(s) for a reply and, if considered appropriate by the editor-in-chief, it will be published as a discussion in a future issue of the journal.

ICE Science journals rely entirely on contributions from the field of materials science and engineering. Information about how to submit your paper online is available at www.icevirtuallibrary.com/page/authors, where you will also find detailed author guidelines.